Antisense morpholino targeting just upstream from a poly(A) tail junction of maternal mRNA removes the tail and inhibits translation

Tadashi Wada[1],*, Masatoshi Hara[2], Takuya Taneda[2], Cao Qingfu[2], Ryouhei Takata[1,3], Kanako Moro[1], Kei Takeda[1,3], Takeo Kishimoto[2] and Hiroshi Handa[2,4],*

[1]Division of Molecular and Cellular Biology, Department of Supramolecular Biology, Graduate School of Nanobioscience, Yokohama City University, Tsurumi-ku, Yokohama, Kanagawa, 230-0045, [2]Graduate School of Bioscience and Biotechnology, [3]Yoshindo Inc. Fuchu-machi, Toyama, 939-2723 and [4]Integrated Research Institute, Tokyo Institute of Technology, Midori-ku, Yokohama 226-8503, Japan

ABSTRACT

Gene downregulation by antisense morpholino oligonucleotides (MOs) is achieved by either hybridization around the translation initiation codon or by targeting the splice donor site. In the present study, an antisense MO method is introduced that uses a 25-mer MO against a region at least 40-nt upstream from a poly(A) tail junction in the 3′-untranslated region (UTR) of maternal mRNA. The MO removed the poly(A) tail and blocked zebrafish *cdk9* (*zcdk9*) mRNA translation, showing functional mimicry between miRNA and MO. A PCR-based assay revealed MO-mediated specific poly(A) tail removal of zebrafish mRNAs, including those for *cyclin B1*, *cyclin B2* and *tbp*. The MO activity targeting *cyclins A* and *B* mRNAs was validated in unfertilized starfish oocytes and eggs. The MO removed the elongated poly(A) tail from maternal matured mRNA. This antisense method introduces a new application for the targeted downregulation of maternal mRNAs in animal oocytes, eggs and early embryos.

INTRODUCTION

The antisense method of gene downregulation classically uses single-stranded (ss) DNA to form a DNA–RNA duplex through complementary base pairing, leading to RNase H-mediated cleavage of the target mRNA *in vivo* (1,2). However, endonucleases exist that efficiently digest ssDNAs, thereby decreasing their antisense activities. Morpholino oligonucleotides (MOs) are frequently used because they are endonuclease resistant (3). In contrast to antisense DNAs that cause target mRNA digestion, MOs do not mediate the RNase H-dependent digestion of mRNAs (3–5). Duplex formation between MOs and mRNA prevents translation through MO hybridization near the mRNA translation initiation codon and disrupts correct splicing by targeting the splice donor site (4,5).

The activation of gene expression coincides with transcriptional activation; gene activation is closely correlated with an increased accumulation of mRNA. However, specialized cells, such as oocytes and neural cells, have a transcription-independent mechanism by which the expression of dormant mRNAs is strictly controlled by specific RNA-binding proteins (6,7). In this mechanism, cytoplasmic elongation of the poly(A) tail leads to translational stimulation of maternal mRNAs in *Xenopus* oocytes and early embryos (6,7).

This article describes a new method for gene downregulation. The availability and specificity were confirmed by targeting the maternal mRNAs of zebrafish *cdk9*, *tbp*, *cyclin B1*, *cyclin B2*, as well as starfish *cyclins A* and *B*. The key features of this method are as follows: (i) duplex formation of the MO with the mRNA 3′-untranslated region (UTR) not only prevents poly(A) tail elongation, but also induces deadenylation like miRNA (8) or removal of the entire tail and (ii) this method blocks target mRNA translation.

MATERIALS AND METHODS

Synthesis

DNA and morpholinos were synthesized by Operon Biotechnologies and Gene Tools, respectively.

Embryos, oocytes and eggs

All zebrafish and embryos were maintained at 28°C and staged as described previously (9). Immature oocytes or

unfertilized mature eggs of the starfish *Asterina pectinifera* were prepared as described (10). Immature oocytes were treated with 1 μM 1-methyladenine (1-MeAde) to induce meiotic maturation at 23°C in artificial seawater (Jamarin Laboratory).

Microinjection of MO

Zebrafish wild-type embryos were injected at the one- or two-cell embryo stage with 2.5 pmol of MO. The MOs used in this study are shown in Supplementary Table S1. When a mixture of two MOs was tested, 1.25 pmol of each MO was injected into the embryo.

Starfish immature oocytes or unfertilized mature eggs were injected with 20 fmol of morpholino antisense oligonucleotides against either starfish *cyclin A* or *B* (Supplementary Table S1). Microinjection was performed as described (11). In Figure 6E, a mixture of sfcycA MO (10 fmol) and sfcycB MO (10 fmol) was used.

Preparation of extracts of embryos, oocytes and eggs

Ten zebrafish embryos were frozen in liquid nitrogen and thawed in 200 μl of RIPA buffer [150 mM NaCl, 1% NP-40, 0.5% deoxycholate, 0.1% sodium dodecyl sulfate, 50 mM Tris–HCl (pH 8.0)]. After thorough sonication, supernatants (100 μl) were collected by centrifugation at 12 000g for 1 min and mixed with 40 μl of 4× Laemmli sample buffer. For western blot analysis, 14 μl of the sample, corresponding to a half-embryo, were analyzed.

Four starfish oocytes were recovered in 5 μl of seawater and 7 μl of 2× Laemmli sample buffer were added for western blot analysis (12).

Purification of total RNA from embryos and oocytes

Total RNA was extracted from 10 zebrafish embryos or 20 starfish oocytes with Sepasol-RNA I super (Nacalai Tesque).

Poly(A) test assays

The PAT assays were performed essentially as described (13), except for minor modifications. Total RNA (300 ng) was incubated at 65°C for 5 min in the presence of a mixture (total 20 ng) of phosphorylated oligo (dT) primers, which were 12- to 18-mer poly (dT) primers. After incubation for 1 h at 42°C with T4 DNA ligase (350 U) (TaKaRa), the samples were further incubated at 12°C for 1 h in the presence of 200 ng (dT)$_{12}$-anchor primer (5′-GCGAGCTCCG CGGCCGCGTT TTTTT TTTT-3′) to generate the 3′-end of the poly (dT) primer, followed by incubation with SuperScript III reverse transcriptase (200 U) (GE Healthcare) for 1 h to make PAT complementary DNAs (cDNAs). Finally, the products of PCR using a gene-specific primer and the (dT)$_{12}$-anchor primer were subjected to 2.2% agarose gel electrophoresis and visualized by ethidium bromide. The gene-specific primers used in this study are shown in Supplementary Table S2.

RT–PCR

RT–PCR was performed with SuperScript III transcriptase (200 U). Random and oligo (dT) primers (Invitrogen) were used as reverse primers. The gene-specific primer sets (forward and reverse primers) used for RT–PCR are shown in Supplementary Table S3.

Western blot analysis

To generate anti-zCdk9 antibodies, the recombinant protein of zCdk9 was expressed in bacteria (*Escherichia coli*) and fractionated by disk preparative electrophoresis. A rabbit was immunized with the Cdk9 protein, according to the standard protocol of Operon Biotechnologies. The polyclonal anti-zCdk9 antibody was affinity purified from the immunoserum as described (14). H-169, which reacted with human Cdk9 and anti-actin (clone C4) antibodies, was purchased from Santa Cruz Biotechnology and Chemicon, respectively. Immunoblotting was performed as described previously (15). Blots were developed with the ECL system (GE Healthcare).

In the case of starfish, the primary antibodies used were anti-starfish cyclin B (10) and anti-MAPK (Upstate), and the secondary antibodies were HRP-conjugated anti-rabbit IgG (GE Healthcare), anti-mouse IgG (Dako) and AP-conjugated anti-rabbit IgG (Dako). Immunocomplexes were detected by the BCIP/NBT phosphatase substrate system (KPL) or ECL Plus (GE Healthcare) and were visualized with LAS4000 IR multi color (Fuji Film).

Determination of the 3′-end sequence of mRNA

We performed reactions according to the manufacturer's manual supplied with the small RNA Cloning Kit (Takara) with minor modifications. Three hundred nanograms of total RNA isolated from embryos were treated with bacterial alkaline phosphatase (BAP). A biotinylated RNA/DNA 3′ adaptor was ligated to the 3′-end of BAP-treated RNA. Streptavidin-conjugated magnetic beads were used to collect the adaptor-ligated RNA. After washing the beads, reverse transcription reactions were performed with PCR-R & RT-primer (5′-GTCTCTAGC C TGCAGGATCG ATG-3′). Synthesized cDNAs were recovered from the beads by alkaline treatment, followed by PCR with *zcdk9* PAT primer and PCR-R & RT-primer. The PCR products were subjected to agarose gel electrophoresis, and DNA bands were visualized by ethidium bromide staining. The bands were cut out, the DNA fragments were eluted and the fragments were cloned into a pMD20-T vector. After blue–white selection of clones on agar plates containing ampicillin, plasmid DNA was recovered from each clone. Insert regions were confirmed by restriction enzyme digestion. More than 10 clones of each sample were selected for further DNA sequencing analysis.

Messenger RNA synthesis and *in vitro* translation

To generate a plasmid for starfish *cyclin B* [pcDNA3sfCycB(XhoI)], a fragment of the starfish *cyclin B* mRNA-coding region was PCR-amplified with the

sfcyclin B Fwd primer (CCGAATTCAT GTCTCTGAG A GTGAGAGG) and the sfcyclin B Rev primer (GGCTC GAGTC AGCAGTTCTC GTCGGCAA) from a cloned starfish cyclin B cDNA (16). This fragment was inserted into EcoRI/XhoI-digested pcDNA3. The EcoRI/ XbaI-digested fragment of pcDNA3sfCycB(XhoI) and the XbaI/ApaI-digested fragment of the zebrafish cyclin B1 3′-UTR, which was PCR-amplified with the zcyclin B1 3′-UTR Fwd primer (GCTCTAGATT GGGGTTA TGC TGAAGAGA) and the zcyclin B1 3′-UTR Rev primer (CCGGGCCCAA AACTTAAAA AGTTTA TT) from zebrafish PAT cDNAs, were inserted into EcoRI/ApaI-digested pcDNA3 to generate the plasmid pcDNA3sfCycBzCycB1 3′-UTR. The ApaI- and XbaI-digested fragments of pcDNA3sfCycBzCycB1 3′-UTR were transcribed *in vitro* with T7 RNA polymerase [T7 mMessage mMachine system (Ambion)]. The synthesized mRNAs were translated *in vitro* with rabbit reticulocyte lysate (Promega) or injected into starfish oocytes and eggs.

RESULTS

Injection of MO targeting the 3′-UTR terminus of *zcdk9* mRNA into zebrafish early embryos inhibits polyadenylation and subsequent translation

While studying the mechanistic aspects of zebrafish kinase *cdk9* mRNA expression at the midblastula transition (17), we noticed that elongation of the poly(A) tail plays a critical role in translation stimulation. To address this finding, we performed an antisense experiment with the low-toxicity nucleoside analogs, MOs (3). We postulated that duplex formation between an MO and the 3′-UTR of mRNA would prevent poly(A) tail elongation. In this study, a nucleotide at the junction of the poly(A) tail is defined as −1, and numbers are assigned as indicated in each figure. The junction information was obtained from the NCBI nucleotide database.

We prepared cdk9 MO consisting of 25 bases that were completely complementary to the terminal sequence of the *zcdk9* mRNA 3′-UTR (Figure 1A). To examine whether MOs against the 3′-UTR affect polyadenylation, a PAT assay (13) was performed, in which the PCR products reflect the poly(A) tail lengths present on a specific mRNA. When injected into fertilized embryos, cdk9 MO markedly reduced the production of slowly migrating bands compared to that of untreated embryos (WT), indicating that cdk9 MO inhibited polyadenylation (Figure 1B). The cdk9 MO also strongly reduced the amount of *cdk9* PCR product, without affecting the products of *tbp* and *cyclin B1*. This result was specific for cdk9 MO, because embryos treated with cdk9m MO carrying 5-base mismatches acted no differently from untreated embryos (Figure 1B). These results suggest that cdk9 MO specifically affects *cdk9* mRNA.

We next assessed the effect of MOs at the protein level. A western blot assay was performed with two independent antibodies, including our original anti-zCdk9 antibody against zebrafish Cdk9 and the commercially available H-169 antibody against human Cdk9. Anti-actin antibodies were used as a control. The cdk9 MO did not affect zCdk9 accumulation in 3 hpf embryos, but blocked the zCdk9 increment that began at 4 h after fertilization (4 hpf) (Figure 1C). In contrast to cdk9 MO, there was no detectable effect of cdk9m MO on *zcdk9* translation. We compared this method with the traditional method targeting the translational start site. Figure 1D shows that this method targeting the 3′-UTR of mRNA works as well as the traditional antisense method. Taken together, these results indicate that the cdk9 MO injection inhibited the translation of *zcdk9* mRNA during early development.

Since the levels of *cdk9* products in the PAT assay were decreased by the injection of cdk9 MO, we next investigated the effect of cdk9 MO using RT–PCR. Reverse transcription was performed with either a random primer or oligo-dT primer, followed by PCR amplification of the *zcdk9*-coding region. To confirm an experimental time course, we examined the expression of the zygotic transcription marker gene, *bilkf*, which was first detected at 3 hpf and began showing mRNA accumulation at 4 hpf (Figure 1E and F) (18). Thus, zygotic transcription appeared to occur at around 3 hpf, corresponding approximately to the beginning of cleavage cycle 10. This result was consistent with previous reports (17–19).

RT–PCR with the random primer yielded the same amount of *zcdk9* products in the RNA of all embryos, regardless of cdk9 MO injection (Figure 1E), which indicates that cdk9 MO did not decrease the amount of *zcdk9* mRNA. In contrast, the oligo-dT primer showed a low-level amplification of *zcdk9* when cdk9 MO-injected embryos were tested (Figure 1F). The oligo-dT primer hybridized with the poly(A) tail, such that the short tail consisting of a few adenosines was insufficient for hybridization and resulted in low amplification. Therefore, the low-level amplification may have been due to poly(A) tail shortening, caused by deadenylation activity (see below). These results indicate that the injection of cdk9 MO into embryos induces deadenylation rather than mRNA degradation.

The active region for polyadenylation by MO exists at 40 nt from the terminus of the *zcdk9* 3′-UTR

To address whether the 3′-UTR terminus plays an important role in MO-mediated repression, three antisense MOs were created, including MO-2 (−26 to −50), MO-3 (−51 to −75) and MO-4 (−76 to −100) (Supplementary Figure S1). The PAT assay and western blot analysis indicated that, of the five MOs listed in Supplementary Figure S1, only cdk9 MO exerted an inhibitory effect on both polyadenylation and translation. This finding suggests that the most terminal portion of the 3′-UTR is critical for inhibition. To verify this result, additional antisense MOs (Figure 2) were created, namely MO-5 (−6 to −30), MO-6 (−11 to −35) and MO-7 (−16 to 40), which showed inhibitory effects on both polyadenylation and translation that were greater than or similar to those of cdk9 MO. A modest effect on both polyadenylation and translation was apparent when MO-8 (−21 to −45) was examined (Figure 2B and C). These results indicate that
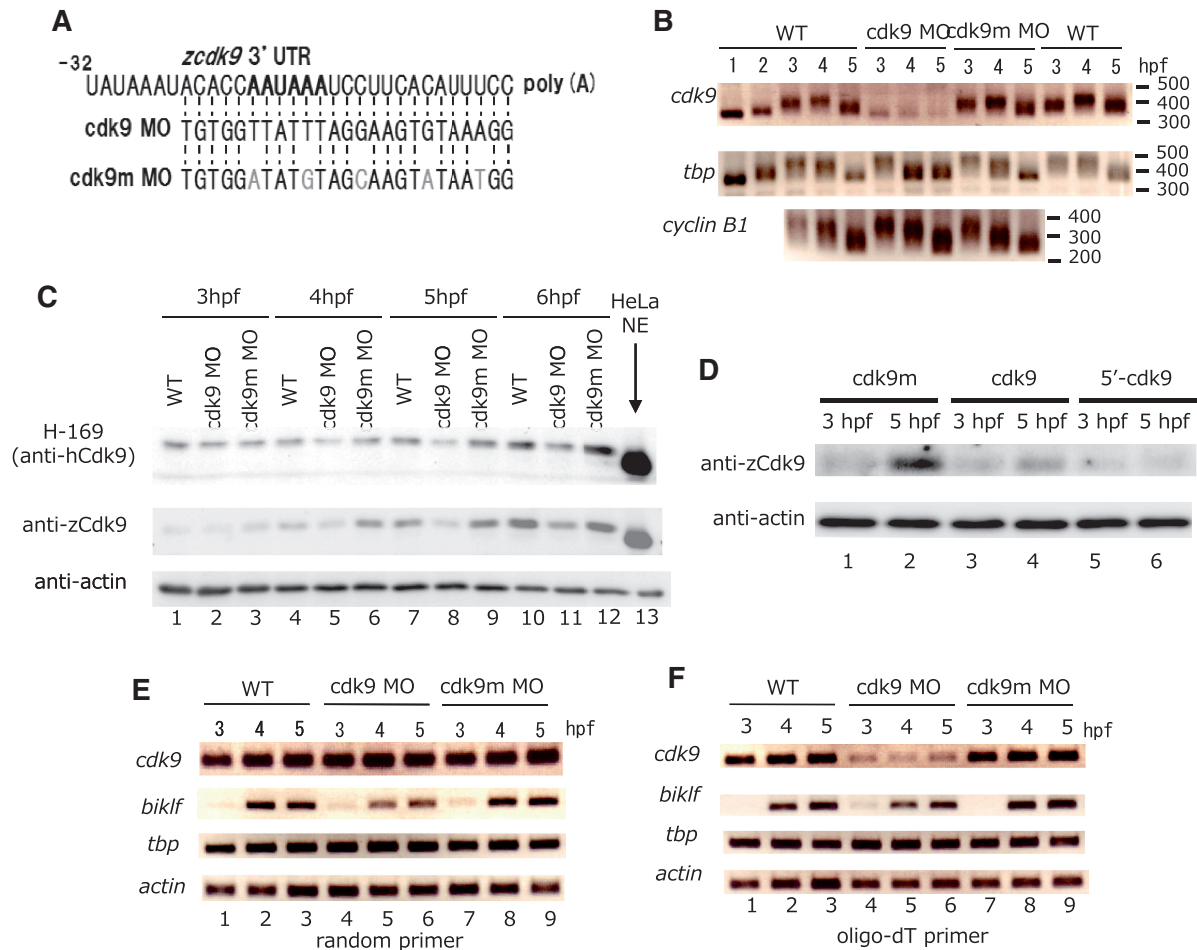
Figure 1. Injection of cdk9, but not cdk9m, MOs into embryos inhibits polyadenylation and translation of *zcdk9* mRNA during early development. (**A**) Target sequence within the *zcdk9* mRNA 3′-UTR and MO hybridization positions. There are five mismatches in cdk9m MO. (**B**) Inhibition of *zcdk9* poly(A) tail elongation in cdk9 MO-injected embryos. Embryos were collected at the times indicated. Total RNA was extracted from untreated (WT), cdk9 MO-injected and cdk9m MO-injected embryos. PAT assay was performed with PAT primers for *cdk9*, *tbp* and *cyclin B1*. PCR products were analyzed on a 2.2% agarose gel. Right side, length markers in bases. (**C**) Specific translation inhibition of *zcdk9* mRNA by cdk9 MO, but not cdk9m MO. Embryos were collected at the indicated times. Western blotting was performed with extracts from untreated (lanes 1, 4, 7 and 10), cdk9 MO-injected (lanes 2, 5, 8 and 11) and cdk9m MO-injected embryos (lanes 3, 6, 9 and 12) by using the antibodies indicated. HeLa cell nuclear extracts (NEs) (lane 13) served as a control. Blots were probed with H-169, anti-zCdk9 and anti-actin. (**D**) The cdk9m MO (lanes 1 and 2), cdk9 MO (lanes 3 1nd 4) and 5′-cdk9 MO targeting a region around the first codon (lanes 5 and 6)-injected embryos were collected at 3 and 5 hpf. The extracts were subjected to western blotting by using antibodies indicated. (**E** and **F**) Reverse transcription using random (E) or oligo-dT primers (F), followed by PCR with primer sets for *cdk9*, *biklf*, *tbp* and *actin*, and analysis on a 2.2% agarose gel. Embryos were collected at the indicated times. Total RNA was extracted from untreated (WT: lanes 1–3), cdk9 MO-injected (cdk9 MO: lanes 4–6) and cdk9m MO-injected embryos (cdk9m MO: lanes 7–9).

the terminal 40 nt of the 3′-UTR act as the active region for MO-mediated inhibition.

Antisense MO removes the poly(A) tail from *zcdk9* mRNA

As shown above, duplex formation of MO with the mRNA 3′-UTR terminus prevents proper polyadenylation. To determine precisely how many adenosine residues remain in the poly(A) tail after injection of MO, we performed DNA sequence analysis of the 3′ region of *zcdk9* cDNAs derived from MO-injected embryos at 3 hpf, similar to those used in Figure 2. The Figure 3A shows a method used in this study. The PCR products were subjected to agarose gel electrophoresis, and DNA

bands were visualized by ethidium bromide (Figure 3B). The PCR products were then cloned into the TA-cloning vector (pMD20-T, TaKaRa) and DNA sequencing analysis of the cloned region was performed.

As shown in Figure 3C, *zcdk9* cDNA derived from MO-2-injected embryos had an intact poly(A) tail, similar to that seen in untreated embryos, In contrast, cDNAs from embryos that had been injected with MO, MO-5, MO-6, MO-7 or MO-8 lost the entire poly(A) tail, indicating that injection of MO into embryos leads to removal of the poly(A) tail from MO-targeting mRNA. Out of the 11 clones in the MO-8 sample, 2 clones had the poly(A) tail region (data not shown).

In addition, the 3′-terminal sequences of the cDNAs were not identical, and the 3′-end residue had moved
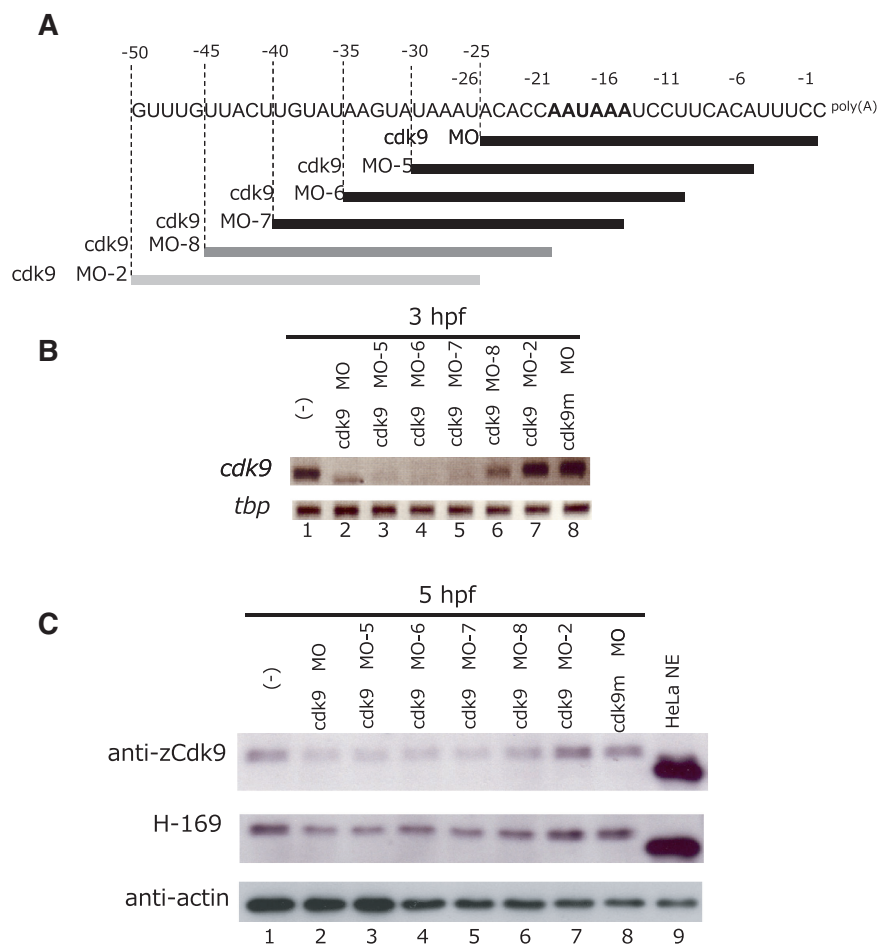
Figure 2. The region 40-nt upstream from the *zcdk9* 3′-UTR end comprises the effective element for MO-mediated repression of *zcdk9* mRNA. (**A**) Terminal sequence of the *zcdk9* mRNA 3′-UTR and hybridization positions of antisense MOs. (**B**) Full repression of *zcdk9* mRNA by injection of cdk9 MO, MO-5, MO-6 and MO-7. Embryos in which indicated MOs were injected (lanes 2 to 8) or uninjected (lane 1) were collected at 3 hpf. The total RNA was extracted, and a PAT assay was performed with PAT primers for *cdk9* and *tbp*. (**C**) Extracts from embryos (5 hpf) in which indicated MOs were injected (lanes 2–8) or uninjected (lane 1) were subjected to 7.5% SDS–polyacrylamide gel electrophoresis. Blots were probed with anti-zCdk9, H-169 and anti-actin. HeLa cell NEs were also analyzed (lane 9) as a control.

upstream relative to the MO-mRNA hybrid position. This tendency of the 3′-end to move upstream was seen with MO, MO-5, MO-6, MO-7 and MO-8. This finding suggests that the hybridization position between MO and mRNA affects the 3′-end determination of each mRNA. This effect may be due to deadenylase and exonuclease activity or to the action of an endonuclease recognizing the hybrid.

Investigation of the effects of MO on four maternal mRNAs

To validate the effect of MO on polyadenylation, three kinds of gene-specific MOs were created, including cyclin B1 MO, cyclin B2 MO and tbp MO, in addition to cdk9 MO (Figure 4). To determine the MO specificity, the total RNA derived from 5 hpf embryos was examined, and a PAT assay was performed (Figure 4B and C). We tested a mixture of cyclin B1 MO plus cyclin B2 MO (Figure 4A and B). Zebrafish has the *cyclin B* orthologs *B1* and *B2*, and their 3′-UTRs exhibit sequence similarity; indeed, there were 10-base homologies between cyclin B1 MO

and cyclin B2 MO (Figure 4A). Cyclin B1 MO and cyclin B2 MO each affected its own target without oligonucleotides interference (Figure 4B). We also observed the specific action of MO when cdk9 MO and tbp MO were examined (Figure 4C). The effects of MO on the polyadenylation of mRNAs were confirmed by using RNA samples collected from 2 to 5 hpf embryos (Supplementary Figure S2A and S2B). In addition, each MO binds to a target 3′-UTR in a specific manner (Supplementary Figure S3). These results indicate that antisense MOs targeting the 3′-UTR of mRNAs affect polyadenylation in early zebrafish embryos in a specific manner.

MO antisense method targeting the 3′-UTR of mRNAs in starfish oocytes: sfcycB MO downregulates expression of *cyclin B* maternal mRNA in a specific manner

Recently, we observed that the poly(A) tail elongation of *cyclins A* and *B* mRNAs during meiotic maturation of oocytes is induced by 1-MeAde (20). Therefore, we verified our method further in starfish. By using the
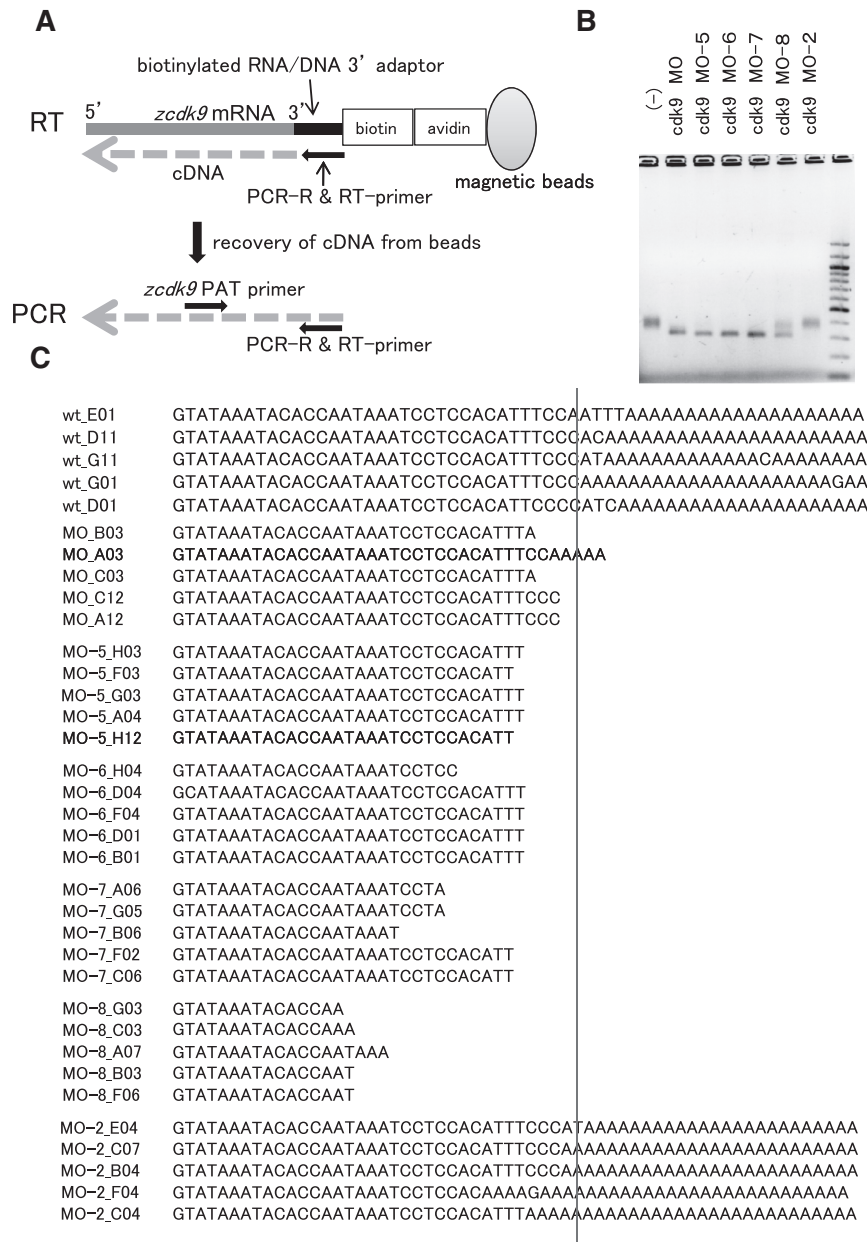
Figure 3. Determination of the mRNA 3′-UTR end. (**A**) Schematic drawings indicate the method employed to determine the mRNA 3′-UTR end. (**B**) Experiments were performed with the total RNA used in Figure 2B. PCR products were visualized by ethidium bromide staining. (**C**) Results of DNA sequencing analysis of each cDNA derived from MO-injected embryos. Five clones were selected and the DNA sequences of their 3′-termini were aligned. A vertical line indicates a poly(A) tail junction of mRNA. The junction information was obtained from the NCBI nucleotide database (NM_212591.1.).

protocol described in Figure 5A, immature oocytes were injected with sfcycB MO and treated with 1-MeAde. We prepared sfcycB MO that has a complementary sequence in its 3′-UTR terminus for starfish *cyclin B* mRNA (Figure 5B), and used cdk9m MO as a control. After meiosis II (MII), total RNA was isolated from oocytes (Figure 5A) and a PAT assay was performed to determine the effect of MO on poly(A) tail elongation. As seen in Figure 5C, 1-MeAde-induced poly(A) tail elongation (∼100 residues) of both maternal *cyclins A* and *B* mRNAs (lanes 2 and 6), and sfcycB MO injection inhibited mRNA polyadenylation of *cyclin B* (lane 7),

but not *cyclin A* (lane 3). Control MO injection did not affect the polyadenylation of either *cyclin A* or *B* mRNAs (lanes 4 and 8). These results indicate that antisense MOs targeting the 3′-UTR of maternal mRNA specifically inhibit polyadenylation in starfish oocytes.

To determine the effect of MO on translation, western blotting was performed with antibodies against the cyclin B protein and MAPK. The 1-MeAde treatment of immature oocytes led to activation of MAPK and cyclic production/degradation of the cyclin B protein (Figure 5F) (10,21). Disappearance of the cyclin B protein at 60 min after 1-MeAde addition and its
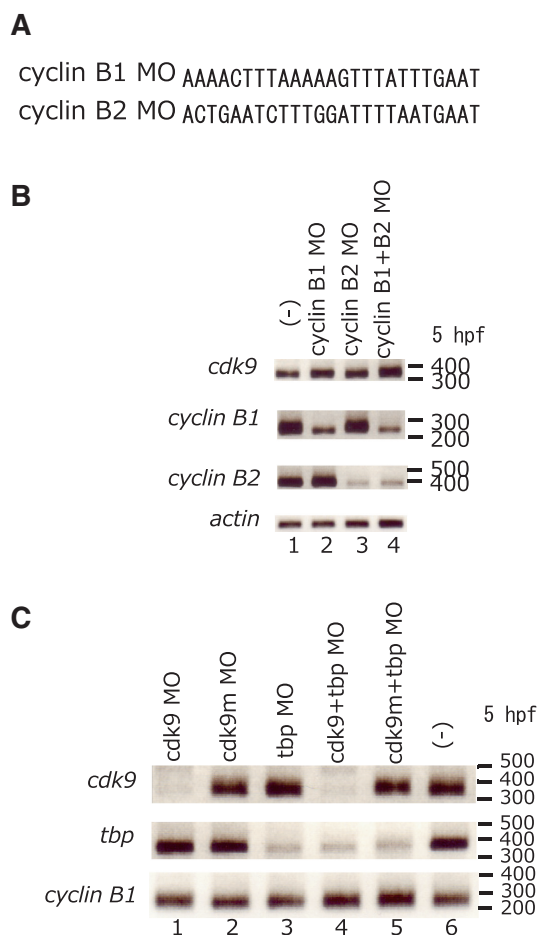
A

cyclin B1 MO AAAACTTTAAAAAGTTTATTTGAAT
cyclin B2 MO ACTGAATCTTTGGATTTTAATGAAT

B

C

Figure 4. Specificity of polyadenylation inhibition by MO. (**A**) Sequences of cyclin B1 and B2 MOs. (**B**) Total RNA was extracted from 5 hpf embryos in which the indicated MOs were injected (lanes 2–4) or uninjected (lane 1). A PAT assay was performed with PAT primers for *cdk9*, *cyclin B1* and *cyclin B2*. PCR using the actin primer set was performed with the cDNA produced in the PAT assay (*actin*). PCR products were analyzed on a 2.2% agarose gel. Right side, length markers in bases. (**C**) Total RNA was extracted from 5 hpf embryos in which the indicated MOs were injected (lanes 1–5) or uninjected (lane 6). A PAT assay was performed with PAT primers for *cdk9*, *tbp* and *cyclin B1*. The PCR products were analyzed on a 2.2% agarose gel. Right side, length markers in bases.

appearance at 70 min indicated that the M phase of MII began ~70 min after 1-MeAde addition (Figure 5F). Furthermore, re-disappearance of cyclin B protein at 90 min indicated an exit from M phase. Importantly, injection of sfcycB MO blocked accumulation of the cyclin B protein at 70 and 80 min (Figure 5F), but the injection of control cdk9m MO did not (data not shown; Figure 5F), which indicates a specific inhibitory effect of sfcycB MO on the translation of maternal *cyclin B* mRNA during MII.

To investigate whether sfcycB MO targets *cyclin B* mRNA in a specific manner, a rescue experiment was performed with *in vitro* synthesized capped mRNAs (Figure 5D). The zebrafish *cyclin B1* 3′-UTR was employed to support the cell cycle-dependent translation of starfish *cyclin B*. The sequence of sfcycB MO did not match a complementary sequence within the zebrafish *cyclin B1* 3′-UTR, suggesting that sfcycB MO cannot

make a duplex with zebrafish *cyclin B1* 3′-UTR. Capped starfish *cyclin B* mRNA lacking the 3′-UTR (Figure 5D) also was prepared. The synthetic individual RNAs were coinjected with sfcycB MO into immature oocytes, and maturation was induced by the addition of 1-MeAde. Western blot analysis showed that the cyclin B proteins were translated efficiently from both synthetic RNAs *in vitro* (Figure 5E). In oocytes, however, the two RNAs exhibited different results. When chimeric mRNA was injected, a significant increase in cyclin B protein accumulation was observed that peaked 70 min after 1-MeAde addition, which was 10 min faster than that of untreated oocytes (Figure 5F). This 10-min difference may be due to the difference in the 3′-UTR between endogenous and injected *cyclin B* mRNAs. Regardless, oocytes produced the cyclin B protein efficiently from the chimeric RNA carrying the zebrafish *cyclin B1* 3′-UTR at MII. In contrast, the *cyclin B* mRNA without the 3′-UTR showed a low level of translation compared to untreated oocytes (Figure 5F), indicating that the 3′-UTR is required for proper *cyclin B* mRNA translation at MII. These results indicate that the zebrafish *cyclin B1* 3′-UTR can partly complement the function of the starfish *cyclin B* 3′-UTR in regulating *cyclin B* mRNA translation during oocyte maturation.

Taken together, these results demonstrate that sfcycB MO downregulates expression of *cyclin B* maternal mRNA in a specific manner.

Duplex formation just upstream of the poly(A) tail induces poly(A) tail deadenylation in mature starfish oocytes

We next examined whether the antisense MO targeting the 3′-UTR of mRNA stimulated deadenylation activity. The protocol shown in Figure 6A was used, because it allowed the injection of MO into pronucleus (PN) stage eggs, in which the cell cycle is arrested at the G1 phase after the completion of MII. Elongation of the poly(A) tail in *cyclins A* and *B* mRNAs occurs during meiotic maturation, and the elongated tails are maintained in arrested oocytes (20).

The sfcycA MO was used against the starfish *cyclin A* 3′-UTR in addition to sfcycB MO (Figure 6B). Eggs (PN_{210}) were collected at 90 min after injection of MO into arrested mature eggs (PN_{120}). The total RNA isolation from the oocytes (Figure 6A) was used in a PAT assay. Both *cyclins A* and *B* mRNAs in mature oocytes had longer poly(A) tails than those of mRNAs in immature oocytes (Figure 6C; lanes 1 and 2), indicating that meiotic maturation induced the poly(A) tail elongation of mRNAs, as we reported previously (20). Injection of sfcycA MO reduced the amount of PCR products from *cyclin A*, but not from *cyclin B*, and sfcycB MO affected only PCR products from *cyclin B* (Figure 6C). In contrast, the control cdk9m MO had no effect on either PCR product. These results indicate that a specific duplex formation upstream of the poly(A) tail leads to poly(A) tail shortening by stimulating deadenylation activity.

Next, we examined whether maternal *cyclins A* and *B* mRNAs carrying shortened poly(A) tails could stimulate
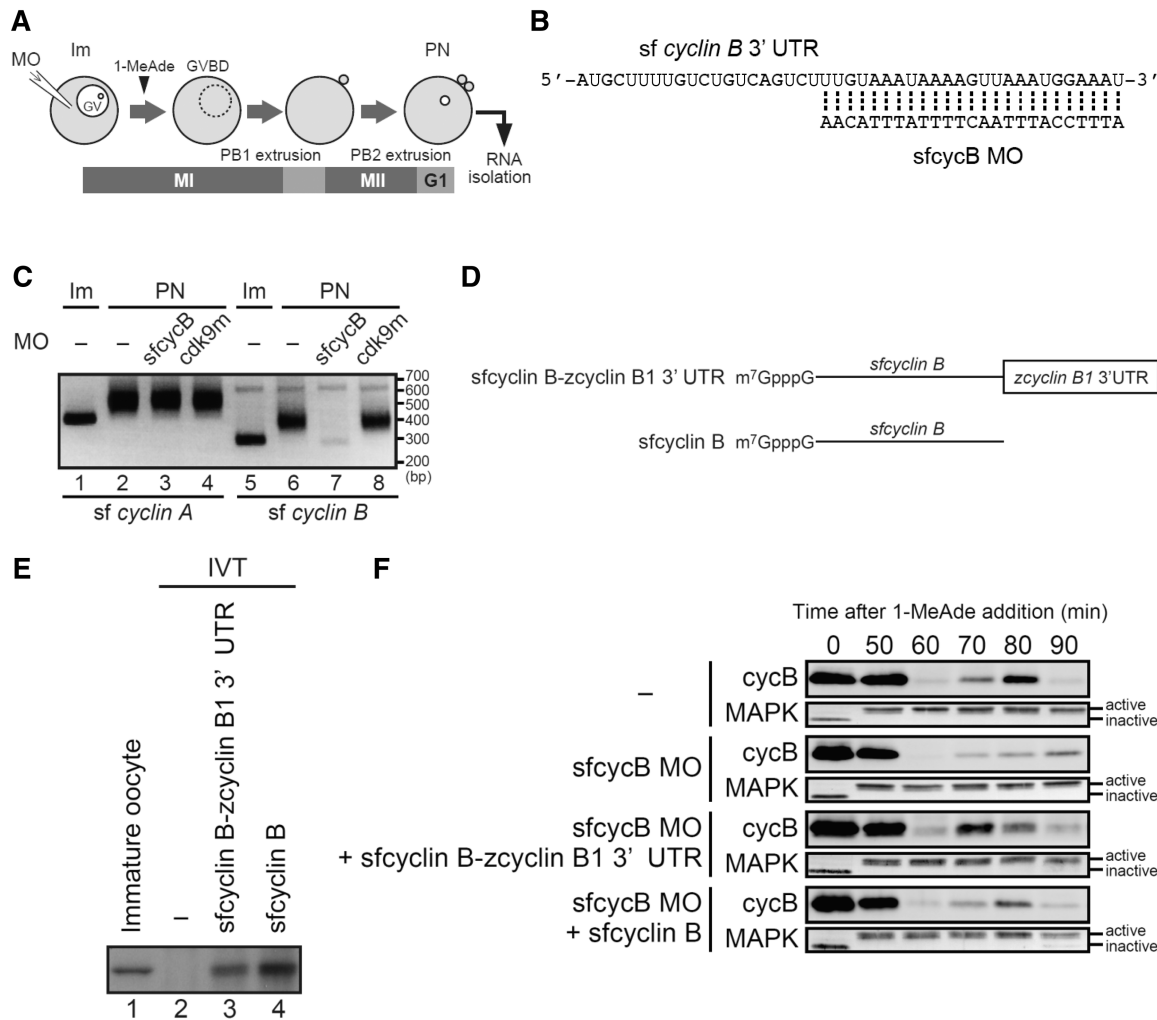
Figure 5. MO-mediated repression and recovery of starfish *cyclin B* mRNA. (**A**) Starfish oocyte maturation and experimental protocol. Immature oocytes (Im) were injected with MO, treated with 1-MeAde and subjected to western blot analysis. To isolate the RNA for the PAT assay in C, oocytes were recovered at 120 min after 1-MeAde treatment (pronuclear stage: PN). (**B**) *Cyclin B* mRNA 3′-UTR sequences adjacent to the poly(A) tail and sfcycB MO. (**C**) sfcycB MO inhibits polyadenylation of *cyclin B*, but not *cyclin A*, mRNAs. Total RNA was isolated from sfcycB MO-injected (lanes 3 and 7), control MO-injected (lanes 4 and 8) or uninjected PN oocytes (lanes 2 and 6), or from uninjected Im oocytes (lanes 1 and 5). Poly(A) tail lengths of *cyclins A* and *B* mRNAs were assessed by PAT. (**D**) Synthetic sfcyclin B mRNAs. sfcyclin B-zcyclin B1 3′-UTR: 5′-capped mRNA comprising the sfcyclin B coding region and zebrafish *cyclin B1* 3′-UTR (upper); sfcyclin B: 5′-capped mRNA comprising the *cyclin B* coding region without the 3′-UTR. (**E**) Chimeric mRNAs in D were translated by *in vitro* translation (IVT) (lanes 3 and 4). Synthesized cyclin B proteins assessed by western blot analysis with anti-cyclin B. Im lysate and IVT without mRNA were used as controls (lanes 1 and 2). (**F**) sfcyclin B-zcyclin B1 3′-UTR, but not sfcyclin B, restores cyclin B protein accumulation following MI exit in sfcycB MO-injected oocytes. Oocytes were injected with sfcycB MO and chimeric mRNA (left), and then were treated with 1-MeAde. Four oocytes were blotted with anti-cyclin B and anti-MAPK.

translation. Eggs were treated with the MAPK inhibitor U0126, which stimulates translation of *cyclins A* and *B* mRNAs (Figure 6D) (20). U0126 inhibited MAPK and stimulated translation in normal eggs (Figure 6E). In contrast, eggs that were injected with a mixture of MOs against *cyclins A* and *B* showed very weak stimulation of translation (compare lanes 3 and 4 in Figure 6E), indicating that MOs targeting the 3′-UTR of mRNAs repress the expression of maternal mRNAs.

DISCUSSION

We report the MO-mediated repression of maternal mRNAs in zebrafish early embryos and starfish oocytes

and eggs. This repression was accomplished by the inhibitions of polyadenylation and translation; however, we do not know whether the same mechanism operates in zebrafish and starfish. Duplex formation of MO with mRNAs at the junction of the poly(A) tail is thought to be necessary for MO-mediated polyadenylation inhibition (Figure 2 and Supplementary Figure S1). Notably, cdk9 MO-2, which possibly hybridizes with the region from 26 to 50 bases upstream from the end of the *zcdk9* 3′-UTR, had no effect on the poly(A) tail (Figures 2 and 3). This result suggests that the responsible *cis*-element(s) exist within 25 bases from the 3′-UTR terminus.

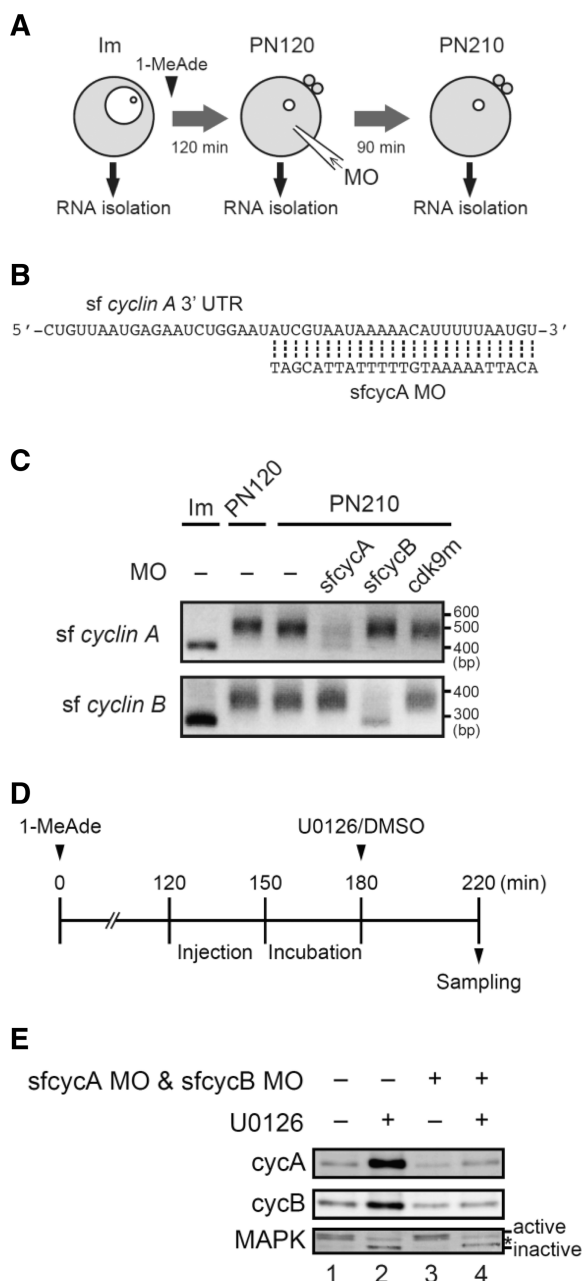Twenty-five bases of *zcdk9*, *cyclins B1* and *B2* mRNAs and 30 bases of *tbp* mRNA have a canonical

Figure 6. MO targeting to the 3′-UTR adjacent to the poly(A) tail induces deadenylation of the target mRNA. (**A**) Schematic representation of the experimental protocol. Im were treated with 1-MeAde. At 120 min later (PN120), oocytes in the pronuclear stage were injected with MO. After 90 min of incubation, the oocytes were recovered and total RNA was isolated (PN210). Total RNA was also isolated from oocytes of Im and PN120 as a control. (**B**) Sequences of the *cyclin A* 3′-UTR adjacent to the poly(A) tail and sfcycA MO. (**C**) sfcycA MO and sfcycB MO cause deadenylation of *cyclins A* and *B* mRNAs, respectively. According to A, total RNA was isolated from uninjected (−), or sfcycA MO-, sfcycB MO- or cdk9m MO-injected (control) oocytes. The poly(A) tail lengths of the *cyclins A* and *B* mRNAs of oocytes were monitored by the PAT assay. (**D**) Experimental schedule. (**E**) The shortened poly(A) tail does not support translation stimulation induced by U0126 addition. According to (D), eggs were injected with a mixture of sfcycA MO and sfcycB MO, treated with U0126 (at a final concentration of 10 μM) and then collected. Four oocytes were prepared for western blot analysis with anti-cyclin B and anti-MAPK antibodies.

polyadenylation signal (AAUAAA) that binds cleavage-polyadenylation specificity factor (CPSF), a component of the cytoplasmic polyadenylation RNP complex (7). In *Xenopus* oocytes, the RNP complex consists of cytoplasmic poly(A) ribonuclease (PARN) and the cytoplasmic poly(A) polymerase (Gld-2), in addition to CPSF and cytoplasmic polyadenylation factors, including CPEB, Pumilio and Musashi (7). Therefore, it is plausible that hybridization of MO to the junction may prevent proper binding of CPSF to the polyadenylation signal, which possibly affects RNP complex function. This process may lead to perturbation of the balance between Gld-2 and PARN activities, resulting in poly(A) tail shortening (22).

Hybridization between MO and mRNA led to removal of the 3′-terminal region and the entire poly(A) tail from mRNA in zebrafish embryos. A few nucleotides at the 3′ region remained just downstream from the hybrid position. Further downstream, nucleotides, including the poly(A) tail, were removed from the mRNA (Figure 3). This removal may be caused by a deadenylase-dependent cutting of the poly(A) tail, followed by exonuclease action to remove several 3′-terminal nucleotides Alternatively, hybridization may stimulate the activity of a certain endonuclease, leading to the digestion of the mRNA at the region just downstream of the hybrid.

There are three important similarities between miRNA and MO behaviors: a target region is located in the 3′-UTR, deadenylation or poly(A) tail removal is induced and translation inhibition occurs (8). It will be of considerable interest to determine the protein components associated with MO-mediated inhibition.

Finally, this method using MO is limited to maternal mRNAs and is not a new tool for repression of gene expression in mammalian cells.

SUPPLEMENTARY DATA

Supplementary Data are available at NAR Online: Supplementary Tables 1–3 and Supplementary Figures 1–3.

Conflict of interest statement. None declared.

REFERENCES

1. Minshull,J. and Hunt,T. (1986) The use of single-stranded DNA and RNase H to promote quantitative 'hybrid arrest of translation' of mRNA/DNA hybrids in reticulocyte lysate cell-free translations. *Nucleic Acids Res.*, **14**, 6433–6451.
2. Cerritelli,S.M. and Crouch,R.J. (2009) Ribonuclease H: the enzymes in eukaryotes. *FEBS J.*, **276**, 1494–1505.
3. Summerton,J. (1999) Morpholino antisense oligomers: the case for an RNase H-independent structural type. *Biochim. Biophys. Acta*, **1489**, 141–158.
4. Eisen,J.S. and Smith,J.C. (2008) Controlling morpholino experiments: don't stop making antisense. *Development*, **135**, 1735–1743.
5. Bill,B.R., Petzold,A.M., Clark,K.J., Schimmenti,L.A. and Ekker,S.C. (2009) A primer for morpholino use in zebrafish. *Zebrafish*, **6**, 69–77.
6. Richter,J.D. (2007) CPEB: a life in translation. *Trends Biochem. Sci.*, **32**, 279–285.
7. Radford,H.E., Meijer,H.A. and de Moor,C.H. (2008) Translational control by cytoplasmic polyadenylation in *Xenopus* oocytes. *Biochim. Biophys. Acta*, **1779**, 217–229.
8. Filipowicz,W., Bhattacharyya,S.N. and Sonenberg,N. (2008) Mechanisms of post-transcriptional regulation by microRNAs: are the answers in sight? *Nat. Rev. Genet.*, **9**, 102–114.
9. Westerfield,M. (1995) *The Zebrafish Book: A guide to the Laboratory Use of Zebrafish (Danio rerio)*, 3 edn. University of Oregon Press, Eugene.
10. Okano-Uchida,T., Sekiai,T., Lee,K., Okumura,E., Tachibana,K. and Kishimoto,T. (1998) In vivo regulation of cyclin A/Cdc2 and cyclin B/Cdc2 through meiotic and early cleavage cycles in starfish. *Dev. Biol.*, **197**, 39–53.
11. Kishimoto,T. (1986) Microinjection and cytoplasmic transfer in starfish oocytes. *Methods Cell Biol.*, **27**, 379–394.
12. Okano-Uchida,T., Okumura,E., Iwashita,M., Yoshida,H., Tachibana,K. and Kishimoto,T. (2003) Distinct regulators for Plk1 activation in starfish meiotic and early embryonic cycles. *EMBO J.*, **22**, 5633–5642.
13. Sallés,F.J. and Strickland,S. (1995) Rapid and sensitive analysis of mRNA polyadenylation states by PCR. *PCR Methods Appl.*, **4**, 317–321.
14. Harlow,E. and Lane,D. (1988) *Antibodies: A Laboratory Manual*. Cold Spring Harbor Laboratory, Cold Spring Harbor, NY.
15. Wada,T., Takagi,T., Yamaguchi,Y., Ferdous,A., Imai,T., Hirose,S., Sugimoto,S., Yano,K., Hartzog,G.A., Winston,F. *et al.* (1998) DSIF, a novel transcription elongation factor that regulates RNA polymerase II processivity, is composed of human Spt4 and Spt5 homologs. *Genes Dev.*, **12**, 343–356.
16. Tachibana,K., Ishiura,M., Uchida,T. and Kishimoto,T. (1990) The starfish egg mRNA responsible for meiosis reinitiation encodes cyclin. *Dev. Biol.*, **140**, 241–252.
17. Kane,D.A. and Kimmel,C.B. (1993) The zebrafish midblastula transition. *Development*, **119**, 447–456.
18. O'Boyle,S., Bree,R.T., McLoughlin,S., Grealy,M. and Byrnes,L. (2007) Identification of zygotic genes expressed at the midblastula transition in zebrafish. *Biochem. Biophys. Res. Comm.*, **358**, 462–468.
19. Mathavan,S., Lee,S.G.P., Mak,A., Miller,L.D., Murthy,K.R.K., Govindarajan,K.R., Tong,Y., Wu,Y.L., Lam,S.H., Yang,H. *et al.* (2005) Transcriptome analysis of zebrafish embryogenesis using microarrays. *PLoS Genet.*, **1**, 260–276.
20. Hara,M., Mori,M., Wada,T., Tachibana,K. and Kishimoto,T. (2009) Start of the embryonic cell cycle is dually locked in unfertilized starfish eggs. *Development*, **136**, 1687–1696.
21. Tachibana,K., Machida,T., Nomura,Y. and Kishimoto,T. (1997) MAP kinase links the fertilization signal transduction pathway to the G1/S-phase transition in starfish eggs. *EMBO J.*, **16**, 4333–4339.
22. Kim,J.H. and Richter,J.D. (2006) Opposing polymerase-deadenylase activities regulate cytoplasmic polyadenylation. *Mol. Cell*, **24**, 173–183.